

# Charge order in $\text{LuFe}_2\text{O}_4$ : antiferroelectric ground state and coupling to magnetism

M. Angst,<sup>1,2,\*</sup> R. P. Hermann,<sup>2,3</sup> A. D. Christianson,<sup>4</sup> M. D. Lumsden,<sup>4</sup> C. Lee,<sup>5</sup> M.-H. Whangbo,<sup>5</sup>  
J.-W. Kim,<sup>6</sup> P. J. Ryan,<sup>6</sup> S. E. Nagler,<sup>4</sup> W. Tian,<sup>1,6</sup> R. Jin,<sup>1</sup> B. C. Sales,<sup>1</sup> and D. Mandrus<sup>1</sup>

<sup>1</sup>*Materials Science and Technology Division, Oak Ridge National Laboratory, Oak Ridge, TN 37831, USA*

<sup>2</sup>*Institut für Festkörperforschung, Forschungszentrum Jülich GmbH, D-52425 Jülich, Germany*

<sup>3</sup>*Department of Physics, B5, Université de Liège, B-4000 Sart-Tilman, Belgium*

<sup>4</sup>*Neutron Scattering Science Division, Oak Ridge National Laboratory, Oak Ridge, TN 37831, USA*

<sup>5</sup>*Department of Chemistry, North Carolina State University, Raleigh, NC 27695, USA*

<sup>6</sup>*Ames Laboratory, Ames, IA 50010, USA*

(Dated: October 21, 2019)

X-ray scattering by multiferroic  $\text{LuFe}_2\text{O}_4$  is reported. Below 320 K, superstructure reflections indicate an incommensurate charge order with propagation close to  $(\frac{1}{3}\frac{1}{3}\frac{2}{3})$ . The corresponding charge configuration, also found by electronic structure calculations as most stable, contains polar Fe/O double-layers with *antiferroelectric* stacking. Diffuse scattering at 360 K, with  $(\frac{1}{3}\frac{1}{3}0)$  propagation, indicates ferroelectric short-range correlations between neighboring double-layers. The temperature dependence of the incommensuration indicates that charge order and magnetism are coupled.

PACS numbers: 71.30.+h, 77.80.-e, 75.80.+q, 61.05.C-

Materials where ferroelectricity or dielectric behavior is coupled to magnetism have the potential for novel applications and are presently receiving a lot of attention [1]. A new type of ferroelectricity, originating from charge order (CO) and seemingly coupled to magnetism, has recently been proposed to occur in  $\text{LuFe}_2\text{O}_4$  containing triangular Fe/O double-layers [2], generating a lot of interest in this material [3, 4, 5, 6, 7, 8]. Ferroelectricity is thought to arise from a particular arrangement of  $\text{Fe}^{2+}$  and  $\text{Fe}^{3+}$  valences within each of the Fe/O double-layers, making these intrinsically polar. However, different reported [8, 9] superstructure reflections indicate an incomplete understanding of the CO, and the full 3D (three-dimensional) charge configuration has yet to be established. The latter determines the stacking of the polarizations of the individual double-layers, and thus the net polarization of the material.

Furthermore, although magnetism in  $\text{LuFe}_2\text{O}_4$  occurs within the charge ordered state there has been no direct observation of coupling between CO and magnetism to date. Such an observation would be an important link in establishing the mechanism by which ferroelectricity, dielectric behavior, and magnetism are coupled via the underlying CO. We have recently grown  $\text{LuFe}_2\text{O}_4$  crystals with magnetic transitions of unprecedented sharpness, on which neutron scattering allowed the first refinement of a 3D spin structure [10].

Here, we present a study of the CO superstructure by synchrotron x-ray scattering. We propose a commensurate approximation for three domains of the incommensurate CO configuration, with propagations close to  $(\frac{1}{3}\frac{1}{3}\frac{2}{3})$ ,  $(\frac{2}{3}\frac{1}{3}\frac{2}{3})$ , and  $(\frac{1}{3}\frac{2}{3}\frac{2}{3})$ , corresponding to an *antiferroelectric* [11] ground state that we also identify by first-principles density-functional theory (DFT) as having the lowest energy. In contrast, short-range charge correlations above the CO temperature were found to correspond to a ferro-

electric CO configuration with  $(\frac{1}{3}\frac{1}{3}0)$  propagation. Furthermore, we provide evidence for a coupling between CO and magnetism involving primarily the incommensuration of the CO. Our results underline the importance of near degeneracy of the CO in  $\text{LuFe}_2\text{O}_4$  and provide an essential microscopic basis for magnetoelectric coupling previously proposed [2, 3, 4, 5].

We studied single crystals from the same batch as those studied in [10]. Specific heat was measured with commercial equipment. X-ray scattering was performed on the (001) surface (in hexagonal notation) of a crystal with a mosaic spread of  $0.02(1)^\circ$  at beam line 6IDB of the Advanced Photon Source, using 16.2 keV photons. All scattered intensities shown are normalized to an ion chamber monitor to account for changes in the incoming beam intensity. Bragg reflections are consistent with the reported structure ( $R\bar{3}m$ ), but the presence of structural reflections, denoted **s**, with comparable intensities following either  $-h + k + l = 3n$  or  $h - k + l = 3n$  ( $n$  integer)  $R$  centering conditions indicates the presence of  $180^\circ$ -twinning, a common defect in  $\text{LuFe}_2\text{O}_4$  [12].

Superstructure reflections (Fig. 1) appear below a sharp feature in the specific heat (inset) at  $T_{CO} \sim 320$  K indicating the CO transition [13]. The indices of the strongest of these reflections are close to  $(\frac{1}{3}\frac{1}{3}\frac{o}{2})$  with  $o$  an odd integer, consistent with [2, 9, 10]. The peaks are sharp along  $hh$ , but broad along  $\ell$ , indicating an out-of-plane correlation length, obtained by the inverse of the full width at half maximum, of  $\xi_c \sim 30$  nm or 35 Fe/O double-layers. Reflections are also present at  $(\frac{1}{3}\frac{1}{3}n)$ , but they are broader with 1 – 2 orders of magnitude lower intensity. We observed incommensurate satellites to  $(00\frac{3o}{2})$  at  $\pm(\tau\tau 0)$ , as in [9], and additionally at equivalent  $\pm(2\tau\tau 0)$  and  $\pm(\tau 2\tau 0)$  [Fig. 2(a)]. Much weaker satellite pairs further occur around  $(\frac{1}{3}\frac{1}{3}\frac{3n}{2})$ , see Fig. 1. As [9], we also observe small systematic deviations of the

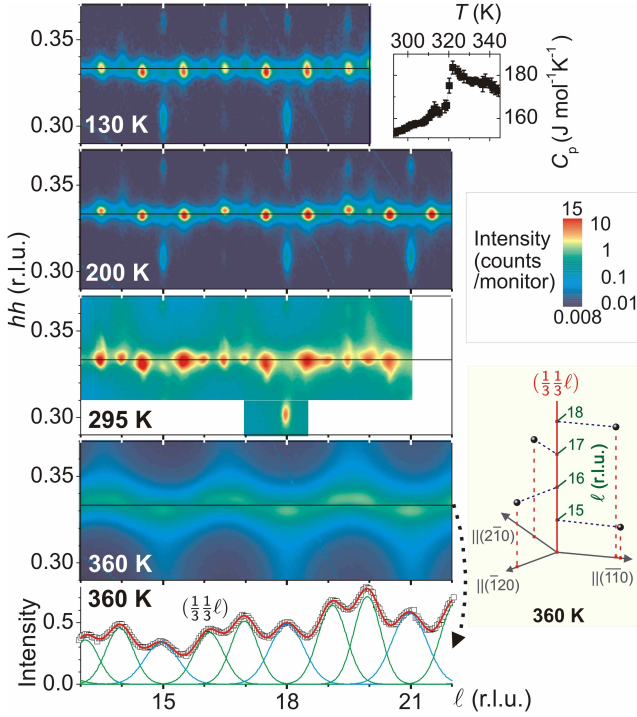


FIG. 1: (Color online) Scattered intensity at  $(hhl)$  at 130, 200, 295, and 360 K. Lowest panel:  $(\frac{1}{3}\frac{1}{3}\ell)$  cut at 360 K with fit by Gaussians. Strong structural reflections reach intensities  $> 10^4$  counts/monitor, strong superstructure reflections  $\sim 40$ . The higher overall intensity at 295 K is due to wider detector slits being used. Horizontal lines mark  $hh = \frac{1}{3}$ . Insets: Specific heat near 320 K; sketch of  $hk\ell$  positions of maxima in diffuse scattering at 360 K.

main reflection maxima from  $hh = \frac{1}{3}\frac{1}{3}$ . For  $\ell \neq 3n$  or  $\frac{3n}{2}$ , this deviation, and the satellites, are out of the  $hhl$  plane,  $\parallel(\bar{2}10)$  or  $\parallel(1\bar{2}0)$  [Fig. 2(c)].

Overall, the observed reflections are consistent with the presence of three domains (labelled A, B, and C hereafter) of CO with the equivalent propagation vectors  $\mathbf{p}_A = (\frac{1}{3} + \delta, \frac{1}{3} + \delta, \frac{3}{2})$ ,  $\mathbf{p}_B = (\frac{2}{3} - 2\delta, \frac{1}{3} + \delta, \frac{3}{2})$ , and  $\mathbf{p}_C = (\frac{1}{3} + \delta, \frac{2}{3} - 2\delta, \frac{3}{2})$ ,  $\delta \sim \tau/10$ , proposed in [9]. The main reflections near  $(\frac{1}{3}\frac{1}{3}\frac{o}{2})$  correspond to  $\mathbf{s} \pm \mathbf{p}_i$ , the broader and weaker  $(\frac{1}{3}\frac{1}{3}n)$  reflections to  $\mathbf{s} \pm 2\mathbf{p}_i$ , with  $\mathbf{s}$  an allowed (see above) structural reflection. The positions and widths of the other reflections are consistent with harmonics of higher order, though the intensity of the satellites around  $(00\frac{3o}{2})$  is surprisingly high [Fig. 2(a)].

To estimate domain populations (and verify propagation type), we collected x-ray diffraction data on a second (untwinned) crystal, using a  $\text{CuK}\alpha$  diffractometer [Fig. 3(a,b)]. Intensities of superstructure reflections close to  $(\frac{1}{3}\frac{1}{3}\frac{o}{2})$  and 3 equivalent directions are shown in Fig. 3(a). Reflections at positions  $\mathbf{s} \pm \mathbf{p}_A$ ,  $\mathbf{s} \pm \mathbf{p}_B$ , and  $\mathbf{s} \pm \mathbf{p}_C$  are indicated by  $\blacksquare$ ,  $\blacktriangle$ , and  $\blacktriangledown$ , respectively. All measurements are consistent with domain A being almost unpopulated, and domain B roughly twice more populated than domain C.

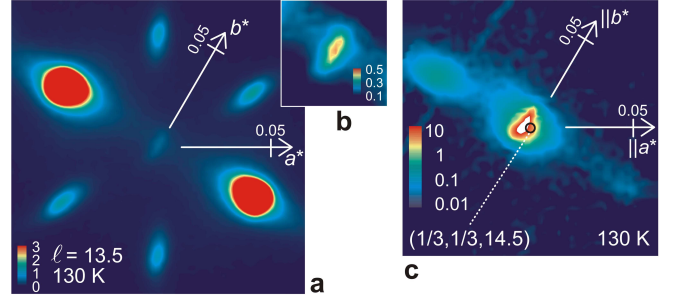


FIG. 2: (Color online) Incommensurate satellites. (a) Intensity at  $(hk13.5)$  at 130 K (the two strongest peaks reach  $\sim 19$  counts/mon). (b) Detail around  $(0,0,13.5)$ . (c) Intensity around  $(\frac{1}{3}\frac{1}{3}14.5)$  (marked by  $\circ$ ).

The intensity ratios of satellite pairs around  $(0,0,19.5)$  [Fig. 3(b)] indicate the same domain populations, supporting the hypothesis that they are related to higher harmonics. Different satellite ring intensity distributions in two samples [Fig. 2(a) and 3(b)], with a strong preference for one direction  $\parallel(\bar{2}10)$  in one, further strongly indicates a single- $\mathbf{k}$  structure within each domain.

To determine the CO configurations corresponding to propagations  $\mathbf{p}_A$ ,  $\mathbf{p}_B$ , and  $\mathbf{p}_C$ , we performed representation analysis [14, 15]. Similar to the spin order determined earlier [10], there are two allowed irreducible CO representations, corresponding to either same or different valence for the 1 and 2 Fe sites [Fig. 3(c,d)] of the primitive (rhombohedral) cell. The former case leads to a CO configuration in which the Fe/O double-layers are not charge neutral. This is physically very unlikely, given the separation of neighboring double-layers by  $\sim 6$  Å. The latter case leads to a single feasible configuration with overall neutral double-layers, see Fig. 3(c). Shown is a commensurate approximation for domain A, accommodated in a  $\sqrt{3} \times \sqrt{3} \times 2$  supercell. In the following, we discuss this commensurate case, which likely [16] describes the CO locally. Due to the atom shifts accompanying the CO [17] the space group symmetry is lowered from rhombohedral  $R\bar{3}m$  to monoclinic  $C2/m$ , and distortions ( $\beta \neq 90^\circ$ ) may be present. To relate the presence or absence of superstructure reflections with the above CO configuration, we calculated their structure factors, as described in [18]. Reflections following  $\mathbf{s} \pm \mathbf{p}_i$  are indeed obtained as principal reflections. In addition, there is a unique set of reflections of the same order of magnitude, at  $\mathbf{s} \pm (00\frac{3}{2})$ , corresponding to the locations around which the ring of strong incommensurate satellites was observed [Fig. 2(a)], consistent with the latter being related to higher harmonics of the same CO as the principal reflections. For completeness, we also calculated the reflection patterns for configurations as proposed in [18] and others corresponding to possible subgroups of  $R\bar{3}m$ , finding all these inconsistent with observation. We therefore conclude that the CO configuration shown in

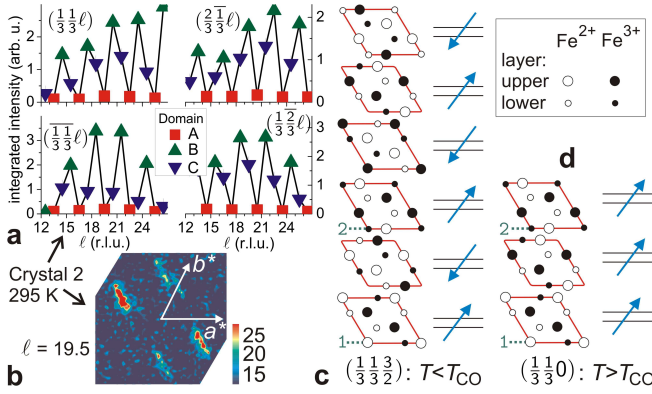


FIG. 3: (Color online) Commensurate approximation of the charge configuration. (a) Integrated intensities of  $(\frac{1}{3}, \frac{1}{3}, l)$  type reflections. Reflections associated with different domains are indicated by different symbols (see text). (b) scattered intensity at  $(hk19.5)$ . (c,d) Charge configuration for domain A for  $T < T_{CO}$  (c) and  $T > T_{CO}$  (d, short-range). Shown are the Fe ions (see legend) of the 6  $(\frac{1}{3}, \frac{1}{3})$  Fe/O double-layers of the  $\sqrt{3} \times \sqrt{3} \times 2$  ( $\times 1$ ) supercell. The direction of the local polarization for each double layer is indicated by an arrow. The two sites of the primitive cell are numbered (see text).

Fig. 3(c) is, apart from domains, the unique solution.

As a further check, we used this solution to re-analyze the 220 K neutron data presented in [10]. Combining the CO model with the previous model of spin order, magnetic scattering at *both*  $(\frac{1}{3}, \frac{1}{3}, n)$  and  $(\frac{1}{3}, \frac{1}{3}, \frac{a}{2})$  could be refined successfully, though with an unexpectedly high magnetic contrast between Fe ions in the two valence states. Details will be given elsewhere.

For the above solution, the configuration in each individual double-layer is as proposed in [2], and thus polar. However, the stacking of the polarization of the six double layers of the supercell [Fig. 3(c)] is *antiferroelectric* with no net polarization. In the previous DFT calculations [6] for the ferroelectric and ferroelectric CO configurations within a  $\sqrt{3} \times \sqrt{3} \times 1$  cell, the latter was found to be more stable than the former, implying that the CO between adjacent Fe/O double layers prefers an antiferroelectric configuration. To confirm this implication, we carried out DFT calculations for the ferroelectric and antiferroelectric CO configurations within a  $\sqrt{3} \times \sqrt{3} \times 2$  cell. Consistent with the experiment, these calculations show that the antiferroelectric CO configuration is more stable than the ferroelectric one [by 3.2 meV/f.u. (formula unit)], and hence corresponds to the ground state.

Our result raises the question how the remanent polarization indicated by pyroelectric current measurements [2] could be explained. A simple explanation would be that the samples are different, since the strong oxygen stoichiometry-dependence of physical properties is well-known. However, this is unlikely to apply, for two reasons. First, superstructure reflections published in the same paper as the polarization results [2] and in several

other papers by the same group (e.g., [9]), are consistent with  $(\frac{1}{3}, \frac{1}{3}, \frac{3}{2})$  propagation. In the above structure factor calculations we found that all investigated CO configurations with non-zero net polarization have  $(\frac{1}{3}, \frac{1}{3}, n)$  reflections at least of the same order of magnitude as  $(\frac{1}{3}, \frac{1}{3}, \frac{a}{2})$  reflections. Second, preliminary pyroelectric current measurements with a similar protocol as in [2] suggest a similar remanent polarization as in [2].

Before presenting an alternative explanation, we turn to the diffuse scattering observed above  $T_{CO}$ . Heating through  $T_{CO}$ , the  $(\frac{1}{3}, \frac{1}{3}, \frac{a}{2})$  and all satellite reflections weaken [Fig. 4(c,d)], as expected, but  $(\frac{1}{3}, \frac{1}{3}, n)$  reflections *gain* in intensity [Fig. 4(b)]. At 360 K there is still considerable diffuse scattering present close to  $(\frac{1}{3}, \frac{1}{3}, l)$ , though with larger deviations from  $\frac{1}{3}$  than at lower  $T$  (Fig. 1). A cut in  $hhl$  along  $(\frac{1}{3}, \frac{1}{3}, l)$  reveals broad maxima now at *integer*  $l$  positions, which are well described by strongly overlapping Gaussians (lowest panel). The precise positions of the diffuse peaks are sketched in an inset to Fig. 1. These peak positions are consistent with  $(\frac{1}{3} - \delta', \frac{1}{3} - \delta', 0)$  propagation and equivalent. The width of the Gaussians in Fig. 1 indicates that CO correlations in  $c$  direction extend to 2–3 double-layers [19], i.e. they are 3D rather than 2D, in contrast to [9]. Representation analysis for the above propagation again yielded two irreducible representations, of which one was rejected as unphysical due to non-charge-neutrality of the double-layers. The remaining representation in commensurate approximation leads to a CO configuration [Fig. 3(d)] with  $\sqrt{3} \times \sqrt{3} \times 1$  cell and ferroelectric stacking of the polarization of the double-layers. Our DFT calculations using the  $\sqrt{3} \times \sqrt{3} \times 2$  cell show that this ferroelectric configuration is less stable than the antiferroelectric configuration (i.e., the ground state), but only by 13.4 meV/f.u.

Although with  $\xi_c \lesssim c$  the description in terms of CO configurations may seem somewhat questionable, the result suggests that the high  $T$  correlations favor a ferroelectric arrangement between neighboring double-layers. It is thus rather surprising that, upon long-range charge ordering, the configuration then established is different and not ferroelectric. Given the small energy-differences between antiferroelectric and ferroelectric configurations of 3% of the overall CO gain, it seems likely that cooling with an electric field applied may stabilize long-range order of the ferroelectric CO configuration, which would explain the remanent polarization observed (only) after cooling in an electric field. This idea should be tested by scattering experiments with electric fields applied in-situ.

In zero electric field, the ground-state has the same *basic* CO configuration with no net polarization at all  $T$  below  $T_{CO}$ , but specific features vary with  $T$ . In this work, we limit our attention to a few selected features, including  $\tau(T)$  [Fig. 4(e)], which is proportional to the fundamental incommensuration of the CO,  $\delta$ , too small to be directly measured. As in  $Fe_2OBO_3$  [16], the incommensuration changes with  $T$ , but it is much smaller and

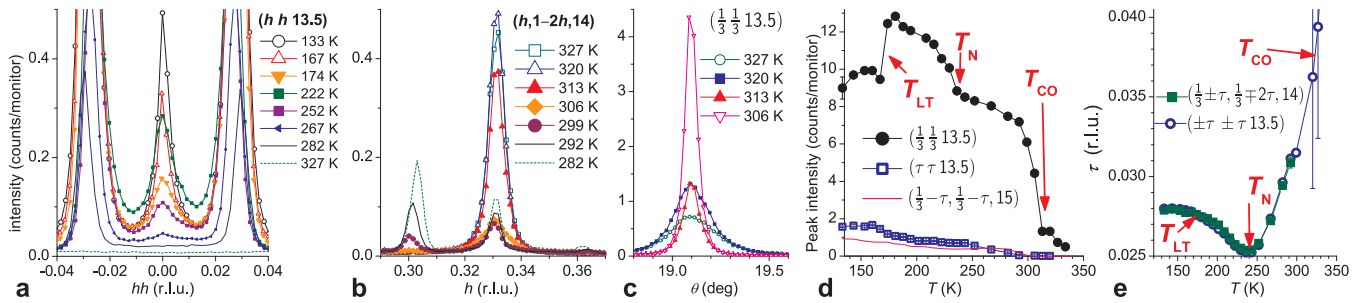


FIG. 4: (Color online)  $T$  dependence of CO on warming. (a)  $(h h 13.5)$  scans. (b) Scans  $\parallel(120)$  through  $(\frac{1}{3} \frac{1}{3} 14)$ . (c)  $(\frac{1}{3} \frac{1}{3} 13.5)$  rocking curves. (d) Peak intensities of three reflections vs  $T$ . (e) Incommensuration  $\tau(T)$ .

present at all  $T$ . In the fluctuation regime,  $\tau$  decreases rapidly upon cooling below  $T_{CO}$ , suggesting that the incommensuration may be an important factor in stabilizing either ferro- or antiferroelectric charge configurations. This trend is reversed at  $T_N \sim 240$  K, where  $\tau(T) \sim 0.025$  has a minimum: The appearance of the magnetic order, which seems to be commensurate [10], results in forcing the CO to become more incommensurate.

In the center of the satellite rings [Fig. 2(a,b)], weak additional reflections develop upon cooling through  $T_N$  [Fig. 4(a)], not likely of magnetic origin. This suggests that the “forced incommensuration” of the CO is somehow compensated by developing a commensurate variant in a small part of the sample. At the low  $T$  transition  $T_{LT} \sim 175$  K reported in [10] the width and intensity of these reflections change [Fig. 4(a)] rapidly compared to other reflections, e.g. no abrupt and little overall change in the intensity of the  $(\frac{1}{3} \pm \tau, \frac{1}{3} \pm \tau, \ell)$  satellites is seen. Yet, for this latter type of reflections the intensity rapidly increased in the previous neutron scattering experiment [Fig. 2(b) of Ref. [10]], implying that the satellites acquire a magnetic moment. Thus, below  $T_{LT}$  the compromise between CO and magnetism involves an incommensurate magnetic structure with compatible propagation vector. The broadness of various magnetic reflections and diffuse magnetic component [Fig. 2(a,c) of [10]] suggests that the “final compromise” below  $T_{LT}$  is more favorable to the CO, given that the CO correlation in  $c$  direction at 130 K is slightly ( $\sim 7\%$ ) improved compared to 200 K.

In conclusion, we show by scattering experiments and DFT calculations that the charge-ordered polar Fe/O double-layers of LuFe<sub>2</sub>O<sub>4</sub> have the antiferroelectric stacking in the ground state. Ferroelectric short-range correlations at high  $T$  revert to this stacking upon long-range ordering. The incommensurate nature of the resulting CO is likely relevant for stabilizing either ferro- or antiferroelectric charge configurations, and it reveals the coupling of the CO to the magnetism, a coupling likely related to the observed [3] large magneto-dielectric effect.

We thank D. S. Robinson for assistance and J. Voigt, H. J. Xiang, H. M. Christen, W. Schweika, A. Kreyssig, Y. Janssen, and S. Nandi for discussions. Work at ORNL, NCSU, and synchrotron work at the MU-CAT

sector of APS was supported by the Division of Materials Sciences and Engineering, Office of Basic Energy Sciences, US Department of Energy (DE-AC05-00OR22725, DE-FG02-86ER45259, DE-ACD02-07CH11358, and DE-AC02-06CH11357).

\* Electronic address: m.angst@fz-juelich.de

- [1] W. Eerenstein, N. D. Mathur, and J. F. Scott, *Nature* **442**, 759 (2006); S.-W. Cheong and M. Mostovoy, *Nat. Mater.* **6**, 13 (2007); M. Bibes and A. Barthélemy, *ibid.* **7**, 425 (2008).
- [2] N. Ikeda *et al.*, *Nature* **436**, 1136 (2005).
- [3] M. A. Subramanian *et al.*, *Adv. Mater.* **18**, 1737 (2006).
- [4] A. Nagano *et al.*, *Phys. Rev. Lett.* **99**, 217202 (2007); M. Naka, A. Nagano, and S. Ishihara, *Phys. Rev. B* **77**, 224441 (2008).
- [5] J. Y. Park *et al.*, *Appl. Phys. Lett.* **91**, 152903 (2007).
- [6] H. J. Xiang and M.-H. Whangbo, *Phys. Rev. Lett.* **98**, 246403 (2007).
- [7] C.-H. Li *et al.*, *Appl. Phys. Lett.* **92**, 182903 (2008).
- [8] Y. Zhang *et al.*, *Phys. Rev. Lett.* **98**, 247602 (2007).
- [9] Y. Yamada *et al.*, *Phys. Rev. B* **62**, 12167 (2000); J. Phys. Soc. Jpn. **66**, 3733 (1997).
- [10] A. D. Christianson *et al.*, *Phys. Rev. Lett.* **100**, 107601 (2008).
- [11] We use the term only to indicate the nature of polar arrangements, not implying reversal of polar arrangements in electric fields, though this seems likely [2] as well.
- [12] Y. Zhang *et al.*, *Phys. Rev. B* **76**, 184105 (2007).
- [13] A freezing of charge hopping around this  $T$  is confirmed by Mössbauer spectroscopy, to be discussed elsewhere.
- [14] A. S. Wills, *Physica B* **276**, 680 (2000); <http://www.chem.ucl.ac.uk/people/wills>.
- [15] W. Sikora, F. Bialas, and L. Pytlík, *J. Appl. Cryst.* **37**, 1015 (2004); <http://www.ftj.agh.edu.pl/~sikora/modyopis.htm>.
- [16] M. Angst *et al.*, *Phys. Rev. Lett.* **99**, 256402 (2007).
- [17] M. Angst *et al.*, *Phys. Rev. Lett.* **99**, 086403 (2007).
- [18] N. Ikeda, S. Mori, and K. Kohn, *Ferroelectrics* **314**, 41 (2005).
- [19] This is a lower limit, because the cut does not go through the peak maxima. Cutting at  $(\frac{1}{3} \frac{1}{3} \ell)$  is the best “compromise” (compare with the sketch in Fig. 1).